Journal of Non-Newtonian Fluid Mechanics, 10 (1982) 185–213
Elsevier Scientific Publishing Company, Amsterdam—Printed in The Netherlands

MATCHED EIGENFUNCTION EXPANSIONS FOR SLOW FLOW OVER A SLOT

S.A. TROGDON * and D.D. JOSEPH

Dept. of Aerospace Engineering and Mechanics, University of Minnesota, Minneapolis, Minnesota 55455 (U.S.A.)

(Received June 24, 1981)

Summary

We solve the problem of plane flow of a second-order fluid over a rectangular slot when inertia is neglected by matching biorthogonal eigenfunction expansions in different regions of flow. The method appears to be cheaper and more accurate than direct numerical methods. The effect of normal stresses on pressure measurements at the bottom of the slot is discussed.

1. Mathematical formulation

We imagine that a non-Newtonian fluid is flowing between two infinitely parallel plates a distance D apart, the bottom plate containing a rectangular slot of height d and width W (see Fig. 1). The origin of coordinates is chosen for convenience to be at the intersection of the centerline of the channel and the centerline of the slot. The flow is a confined flow and therefore velocities will be specified everywhere on the boundary. It will be assumed that the flow is plane and steady, that the fluid is incompressible and that body and inertial forces are negligible. Given these assumptions, the equations and boundary conditions governing the motion of the fluid are given by:

$$\begin{aligned} &\operatorname{div} \hat{\boldsymbol{T}} = \operatorname{div} \hat{\boldsymbol{u}} = 0 \text{ in } \hat{\Omega}, \\ &\boldsymbol{u} \text{ given on } \partial\hat{\Omega}, \end{aligned} \tag{1.1}$$

* Dept. of Mechanical Engineering, Clarkson College, Potsdam, New York 13676.

0377-0257/82/0000–0000/$02.75

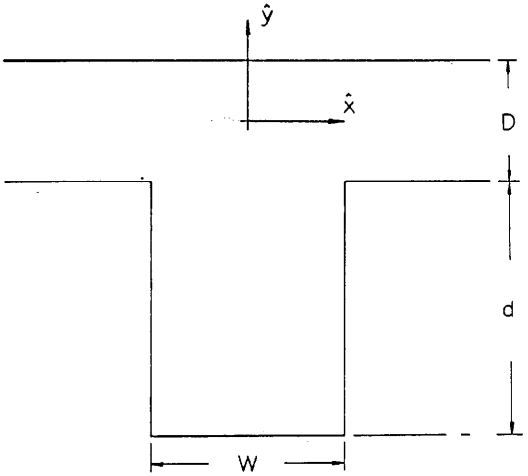

Fig. 1. Domain for flow over a rectangular slot.

where the domain, $\hat{\Omega}$, and its boundary, $\partial\hat{\Omega}$, are shown in Fig. 1. The Cauchy stress, $\hat{\boldsymbol{T}}$, is given by

$$\hat{\boldsymbol{T}} = -\hat{\Phi}\boldsymbol{I} + \mu\hat{\boldsymbol{A}}_1 + \alpha_1\hat{\boldsymbol{A}}_2 + \alpha_2\hat{\boldsymbol{A}}_1^2, \tag{1.2}$$

where $\hat{\Phi}$ is the pressure and $\hat{\boldsymbol{A}}_1$ and $\hat{\boldsymbol{A}}_2$ are the first two Rivlin–Ericksen Tensors and are given by

$$\hat{\boldsymbol{A}}_1 = \operatorname{grad}\hat{\boldsymbol{u}} + (\operatorname{grad}\hat{\boldsymbol{u}})^{\mathrm{T}},$$

$$\hat{\boldsymbol{A}}_2 = \frac{\mathrm{d}\hat{\boldsymbol{A}}_1}{\mathrm{d}t} + \hat{\boldsymbol{A}}_1(\operatorname{grad}\hat{\boldsymbol{u}}) + (\operatorname{grad}\hat{\boldsymbol{u}})^{T}\hat{\boldsymbol{A}}_1.$$

Equation $(1.1)_2$ along with the assumption of plane flow implies the existence of a streamfunction, $\hat{\Psi}(\hat{x}, \hat{y})$. The $\hat{x}$-velocity, $\hat{u}$ and the $\hat{y}$-velocity, $\hat{v}$ are given through the streamfunction by

$$(\hat{u}, \hat{v}) = \left(\hat{\Psi}_{\hat{y}}, -\hat{\Psi}_{\hat{x}}\right).$$

Thus,

$$[\hat{\boldsymbol{A}}_1] = \begin{bmatrix} \hat{\delta} & \hat{\gamma} \\ \hat{\gamma} & -\hat{\delta} \end{bmatrix}$$

where

$$\hat{\delta} = 2\hat{\Psi}_{\hat{x}\hat{y}},$$

$$\hat{\gamma} = \hat{\Psi}_{\hat{y}\hat{y}} - \hat{\Psi}_{\hat{x}\hat{x}},$$

and

$$\hat{\boldsymbol{A}}_1^2 = (\hat{\delta}^2 + \hat{\gamma}^2)\boldsymbol{I}$$

where

$$[\boldsymbol{I}] = \begin{bmatrix} 1 & 0 \\ 0 & 1 \end{bmatrix}$$

If we define

$$\hat{\boldsymbol{S}} \equiv \hat{\boldsymbol{T}} + \hat{\Phi}\boldsymbol{I},$$

the components of $\hat{\boldsymbol{S}}$ are given by

$$\hat{S}\langle xx\rangle = \mu\hat{\delta} + \alpha_1\left[\hat{\Psi}_{\hat{y}}\hat{\delta}_{\hat{x}} - \hat{\Psi}_{\hat{x}}\hat{\delta}_{\hat{y}} + \hat{\delta}^2 - 2\hat{\gamma}\hat{\Psi}_{\hat{x}\hat{x}}\right] + \alpha_2(\hat{\delta}^2 + \hat{\gamma}^2),$$

$$\hat{S}\langle yy\rangle = -\mu\hat{\delta} + \alpha_1\left[\hat{\Psi}_{\hat{x}}\hat{\delta}_{\hat{y}} - \hat{\Psi}_{\hat{y}}\hat{\delta}_{\hat{x}} + \hat{\delta}^2 + 2\hat{\gamma}\hat{\Psi}_{\hat{y}\hat{y}}\right] + \alpha_2(\hat{\delta}^2 + \hat{\gamma}^2),$$

$$\hat{S}\langle xy\rangle = \hat{S}\langle yx\rangle = \mu\hat{\gamma} + + \alpha_1\left\{\left(\hat{\Psi}_{\hat{y}}\frac{\partial}{\partial\hat{x}} - \hat{\Psi}_{\hat{x}}\frac{\partial}{\partial\hat{y}}\right)\hat{\gamma} + \hat{\delta}\,\hat{\nabla}^2\hat{\Psi}\right\}. \tag{1.3}$$

By Tanner's [1] theorem, $\hat{\Psi}$ satisfying

$$\hat{\nabla}^4\hat{\Psi} = 0 \text{ in } \hat{\Omega},$$

$$\left(\hat{\Psi},\ \frac{\partial\hat{\Psi}}{\partial n}\right) \text{ given on } \partial\hat{\Omega}, \tag{1.4}$$

where $\dfrac{\partial}{\partial n}$ is a derivative in the direction of the outward normal and

$$\hat{\nabla}^4 = \frac{\partial^4}{\partial\hat{x}^4} + 2\frac{\partial^4}{\partial\hat{x}^2\partial\hat{y}^2} + \frac{\partial^4}{\partial\hat{y}^4},$$

leads, through (1.3), to a unique [2] Stokes flow solution $(\hat{u}, \hat{v})$ with a non-Newtonian pressure [3,4]

$$\hat{\Phi} = \hat{\Phi}_0 + \left(\frac{\alpha_1}{\mu}\right)\frac{\mathrm{d}\hat{\Phi}_0}{\mathrm{d}t} + \frac{1}{2}\left(\alpha_2 + \frac{3\alpha_1}{2}\right)\operatorname{tr}\hat{\boldsymbol{A}}_1^2, \tag{1.5}$$

where $\hat{\Phi}_0$ is the Newtonian pressure determined by the solution of the Stokes flow problem

$$\operatorname{grad}\hat{\Phi}_0 = \mu\operatorname{div}\hat{\boldsymbol{A}}_1. \tag{1.6}$$

Since Stokes flows are reversible flows and since the domain, $\hat{\Omega}$, is symmetric about the centerline of the slot, uniqueness implies that the streamfunction, $\hat{\Psi}$, is even in $\hat{x}$,

$$\hat{\Psi}(-\hat{x}, \hat{y}) = \hat{\Psi}(\hat{x}, \hat{y}) \tag{1.7}$$

and the Newtonian pressure, $\hat{\Phi}_0$, is odd in $\hat{x}$

$$\Phi_0(-\hat{x},\hat{y}) = -\Phi_0(\hat{x},\hat{y}) \tag{1.8}$$

when as $\hat{x} \to \pm\infty$ the flow is rectilinear and symmetric:

$$\hat{\Psi}(\hat{x},\hat{y}) \to \hat{f}(\hat{y}) \quad \text{as } \hat{x} \to \pm\infty, \tag{1.9}$$

where

$$\hat{\nabla}^4 \hat{f} = 0.$$

The assumption (1.9) will thus accommodate either pressure driven or shear (top plate moving) flows or a combination of both.

2. The hole error

It was first suggested by Broadbent et al. [5] that the normal stress measured on the bottom of a slot for a viscoelastic fluid deviated from the pressure on that boundary (see also [3]). More recently devices have been built (e.g. Seiscor–Lodge Stressmeter [6]) which exploit this deviation and purport to measure elastic properties of fluids. Therefore, from a practical point of view, it would seem desirable to be able to predict exactly how the flow, and in particular how the stresses, depend upon the viscoelastic parameters, α_1 and α_2, appearing in eqn. (1.2).

Using (1.2) and (1.5) and evaluating $\hat{T}\langle yy\rangle$ on a stationary boundary the reader may verify that

$$\hat{T}\langle yy\rangle = -\hat{\Phi}_0 + \frac{\alpha_1}{2}\left(\frac{\partial \hat{u}}{\partial \hat{y}}\right)^2. \tag{2.1}$$

Two flows of interest are the pressure driven flow and the shear driven flow. The hole pressure P_e, is more interesting in the pressure driven case and will be defined as

$$P_e = \frac{\left[\hat{T}\langle yy\rangle|_{\hat{y}=D/2} - \hat{T}\langle yy\rangle|_{\hat{y}=-D/2-d}\right]_{\hat{x}=0}}{\left[\frac{\partial \hat{u}}{\partial \hat{y}}\right]^2|_{\hat{y}=-D/2,\hat{x}=\pm\infty}}. \tag{2.2}$$

Because the Newtonian pressure, $\hat{\Phi}_0$, is a constant along the centerline of the slot (see [4]), the hole pressure in the pressure driven case may be expressed in terms of velocity gradients. Thus,

$$\frac{P_e}{\frac{1}{2}\alpha_1} = \frac{\left[\left(\frac{\partial \hat{u}}{\partial \hat{y}}\right)^2|_{\hat{y}=D/2} - \left(\frac{\partial \hat{u}}{\partial \hat{y}}\right)^2|_{\hat{y}=-D/2-d}\right]_{\hat{x}=0}}{\left(\frac{\partial \hat{u}}{\partial \hat{y}}\right)^2|_{\hat{y}=-D/2,\hat{x}=\pm\infty}}.$$

Given the solution $\hat{\Psi}$ of (1.4) we can compute $\partial \hat{u}/\partial \hat{y} = \hat{\Psi}_{\hat{y}\hat{y}}$ and hence $2P_e/\alpha_1$. It is well-known that (1.2) is a valid asymptotic form of the constitutive equation for simple fluids with fading memory in slow flow. If we assume that inertia is negligible, then (1.1) holds and α_1 may be determined from the experimentally determined values of P_e.

The normal stress contribution to the hole pressure is governed by (1.1) asymptotically as the slot width W tends to zero. The velocity which drives the motion in the slot is the velocity at the slot entrance and this velocity must vanish at the corners. A representative scale velocity is the value $\hat{u}(0, -D/2)$ of $\hat{u}(\hat{x}, \hat{y})$. This is given roughly by $\hat{u} \simeq \tau W$ where τ is the undisturbed shear stress at the channel wall ($y = -D/2$) and $\hat{u}$ is small when W is. In the limit as $\hat{u}$ tends to zero the inertial terms tend to zero like $\rho \hat{u}^2/W$ and the normal stresses like $\alpha \hat{u}^2/W^3$, so that the ratio

$$\frac{\text{inertia}}{\text{normal stress}} \to \frac{\rho}{\alpha} W^2 \quad \text{as} \quad W \to 0,$$

where α is a normal-stress coefficient (see (1.2)). In fact, when W is not small, the observed flow in the slot is not symmetric even when the flow in the channel is slow [7,8]. Some additional comments about the observed asymmetry of flow are reviewed in the Appendix.

3. Comparison of methods of solution

Many numerical methods have been used to solve the problem of flow over a slot. O'Brien [9], using finite differences, solved the problem for different types of upstream velocity profiles (e.g. parabolic and linear). Townsend [10] has extended O'Brien's work, using finite differences to analyze the pressure driven flow of a second order fluid, when inertia is included. The immediate application of his work is to the Seiscor–Lodge Stressmeter. Malkus [11] has used finite elements in analyzing the problem (1.4) and Mir-Mohamad-Sadegh and Rajagopal [12] have used a boundary integral approach to analyze the same problem. Recently, Cochrane, Walters and Webster [13] have numerically simulated the behavior of both Newtonian and elastic liquids in a number of complex geometries, one of these geometries being the slot. They use a finite difference approach to solve the equations of motion. The difference between their work and that of Townsend [10] is that instead of a Rivlin–Erickson model they use a Maxwell model to express the dependence of the Cauchy stress on kinematical quantities. In addition to numerical simulation they have some excellent flow visualization photographs of the simulated flows. They observe that for flow across a slot, inertial effects tend to destroy the symmetry of flow and that the presence of fluid elasticity tends to compete with fluid inertia to restore

the symmetry lost by the presence of inertia alone. In Fig. 2 we have exhibited a photograph of theirs for the case $Re = 1$ and $\lambda = 0$ where λ is a relaxation time to be associated with fluid elasticity ($\lambda = 0$ for a Newtonian liquid). This photograph is the one closest to the Stokes flow limit and it looks very much like our Fig. 8 except the center of the vortex in the cavity in their photograph is positioned lower in the cavity than what we computed numerically. This discrepancy is also noted by them relative to their numerical simulations. They observe that the presence of fluid elasticity tends to push the channel flow deeper into the cavity.

All of the above analyses require some discretization of either the domain of flow or its boundary. In addition one must choose approximating functions for the discretized domain in the finite element approach, decide how to approximate derivatives in the finite difference approach and make assumptions as to the behavior of fictitious source points on the discretized boundary in the boundary integral approach. A method which avoids, to a large extent, all of the above approximations is the method of matched eigenfunction expansions. To implement the method the domain of flow is broken up into several sub-regions. Over each sub-region the solution is sought as a finite sum over a complete set of eigenfunctions. The solutions are then matched along their common boundaries. There is no real discretization of the domain of flow or its boundary. The dependence of the solution on the size of the sub-regions is taken up in eigenvalues which are

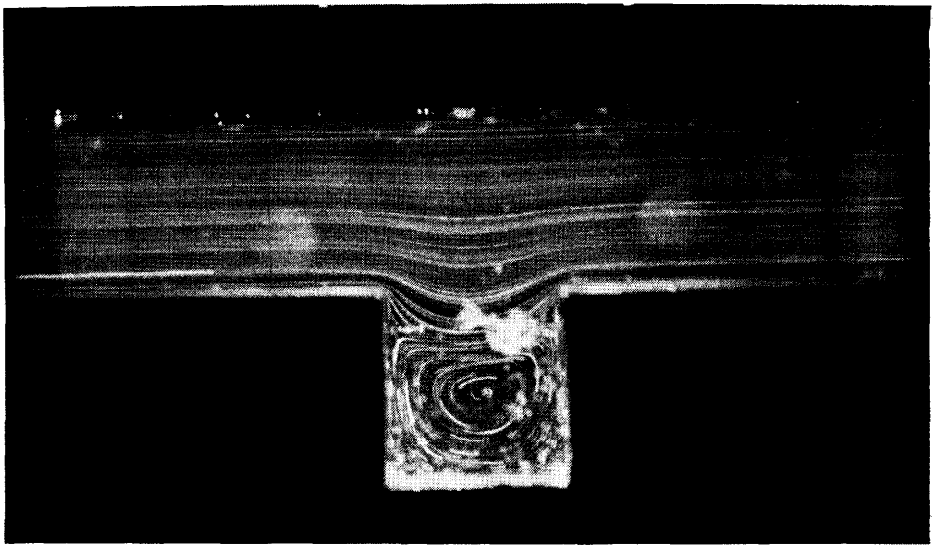

Fig. 2. Photograph showing streamlines for flow over a slot ($Re=1$, $\lambda=0$). Photograph courtesy Cochrane, Walters and Webster, Fig. 5a.

induced by separating variables. Thus changing the overall geometry will change the geometry of each sub-region and hence change the eigenfunction representations for each sub-region.

In the problem of flow in a wedge Sanders, O'Brien and Joseph [14] have shown that the eigenfunction method is much more accurate and much less expensive than finite differences.

4. Eigenfunction solutions

We are interested in solving problem (1.4). We write this problem again, now in dimensionless variables with lengths expressed in units of $D/2$ and $\hat{\Psi}$ in units of Q, the flow rate. Thus,

$$\nabla^4 \Psi = 0 \quad \text{in } \Omega,$$
$$\left.\begin{matrix} \Psi \\ \dfrac{\partial \Psi}{\partial n} \end{matrix}\right\} \text{specified on } \partial\Omega, \tag{4.1}$$

where $\dfrac{\partial}{\partial n}$ is a derivative in the direction of the outward normal and the domain, Ω and its boundary, $\partial\Omega$ are shown in Fig. 3. As $x \to \infty$, $\Psi \to f(y)$ and $\Psi(-x, y) = \Psi(x, y)$.

Solutions of (4.1) will be expressed in series of Papkovich–Fadle eigenfunctions. These eigenfunctions arise from separation of variables in a natural way. This elementary method of solution was first used for a Stokes flow problem in slots by Joseph and Sturges [15,16]. The method has a long

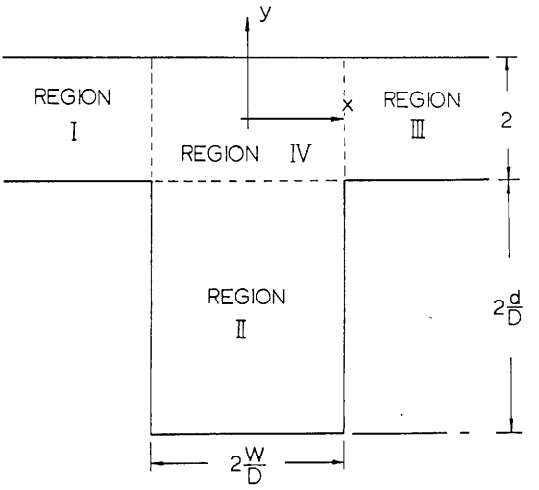

Fig. 3. Domain for flow over a rectangular slot in dimensionless coordinates showing the four sub-regions of flow.

history in elasticity. A particularly notable contribution was made by Smith [17]. Smith proved completeness in an overly restricted class of functions (completeness means convergence of the series to prescribed data). Joseph [18] extended the completeness proof of Smith to classes of data which do arise in applications. The recent completeness proofs of Gregory [19,20,21] and Spence [22] relax the assumptions about the data still further.

In this paper we use notations introduced by Smith [17] and we refer the reader to the papers of Joseph and Sturges [15,16] for further information about the eigenfunction expansions.

Now we shall piece together eigenfunction solutions which are valid in different regions of the flow. The method of matching used to join solutions seems to have been used first by Zidan [23] to solve the problem of extrusion of a low speed jet from a pipe. His solution failed because the set of eigenfunctions he used was not complete in the region occupied by the jet. The method of matching was successfully used first by Sturges [24] and more recently by Trogdon and Joseph [25] to solve different versions of the same extrusion problem. The present application is novel because the geometry of the flow is more complicated.

We shall proceed as follows. In this section we shall list the solutions. Without further discussion the reader may easily verify that the listed solutions are biharmonic and satisfy the boundary conditions. The matching or joining conditions are discussed in the next section.

The domain of flow, Ω, is divided into four sub-regions as shown in Fig. 3. The solution in region I is of the form

$$\Psi^{\mathrm{I}}(x,y) = f(y) + \sum_{-\infty}^{\infty} \frac{C_k}{P_k^2}\phi_k(y)\, \mathrm{e}^{P_k(x+W/D)} + \sum_{-\infty}^{\infty} \frac{C_k^*}{P_k^{*2}}\phi_k^*(y)\, \mathrm{e}^{P_k^*(x+W/D)}, \tag{4.2}$$

where

$$\phi_k(s) = P_k[\sin P_k \cos P_k s - s \cos P_k \sin P_k s],$$

P_k being the 1st quadrant roots of

$$\sin 2P_k + 2P_k = 0, \quad |P_1| < |P_2| < \ldots < |P_k|, \quad P_{-k} = \bar{P}_k$$

and

$$\phi_k^*(s) = P_k^*[\cos P_k^* \sin P_k^* s - s \sin P_k^* \cos P_k^* s],$$

P_k^* being the 1st quadrant roots of

$$\sin 2P_k^* - 2P_k^* = 0, \quad |P_1^*| < |P_2^*| < \ldots < |P_k^*|, \quad P_{-k}^* = \bar{P}_k^*.$$

The solution in region III is the same as the solution in region I,

$$\Psi^{\mathrm{III}}(x,y) = \Psi^{\mathrm{I}}(-x,y). \tag{4.3}$$

The solution in region I must be joined to the solution in region IV on the line $x = -W/D$.

In region II the solution takes the form

$$\Psi^{II}(x,y) = \sum_{-\infty}^{\infty} \frac{D_k}{\hat{P}_k^2} \hat{\phi}_k(x)\, e^{\hat{P}_k(y+1)} + \sum_{-\infty}^{\infty} \frac{E_k}{\hat{P}_k^2} \hat{\phi}_k(x)\, e^{-\hat{P}_k(y+1+2d/D)} \tag{4.4}$$

where

$$\hat{\phi}_k(s) = \phi_k\left(\frac{s}{W/D}\right),$$

$$\sin 2\hat{P}_k W/D + 2\hat{P}_k W/D = 0$$

and thus,

$$\hat{P}_k = \frac{P_k}{W/D}.$$

The solution in region II must be joined to the solution in region IV on the line $y = -1$.

In region IV we have four independent biharmonic series of eigenfunctions at our disposal

$$\begin{aligned} \Psi^{IV}(x,y) = f(y) \quad &+ \sum_{-\infty}^{\infty} \frac{Q_k}{P_k^2} \phi_k(y) \frac{\cosh P_k x}{\cosh P_k W/D} \\ &+ \sum_{-\infty}^{\infty} \frac{Q_k^*}{P_k^{*2}} \phi_k^*(y) \frac{\cosh P_k^* x}{\cosh P_k^* W/D} \\ &+ \sum_{-\infty}^{\infty} \frac{A_k}{\hat{P}_k^2} \hat{\phi}_k(x) \frac{\sinh \hat{P}_k y}{\sinh \hat{P}_k} \\ &+ \sum_{-\infty}^{\infty} \frac{B_k}{\hat{P}_k^2} \hat{\phi}_k(x) \frac{\cosh \hat{P}_k y}{\cosh \hat{P}_k}. \end{aligned} \tag{4.5}$$

It is easy to verify that (4.2), (4.4) and (4.5) are biharmonic.

We now relate the coefficients in the expansions to prescribed conditions on the boundary. In region I, (4.3) satisfies the boundary conditions identically. Equation (4.4) satisfies the boundary conditions at $x = \pm W/D$ and will satisfy the conditions on the bottom of the slot, $y = -1 - 2d/D$, if

$$\Psi^{II}(x, -1-2d/D) = 0 \tag{4.6}_1$$

and

$$\frac{\partial \Psi^{II}}{\partial y}(x, -1-2d/D) = 0. \tag{4.6}_2$$

The solution (4.5) in region IV will satisfy the boundary conditions on the top of the channel, $y = 1$, if

$$\Psi^{IV}(x, 1) = f(1) \tag{4.7}_1$$

and

$$\frac{\partial \Psi^{IV}}{\partial y}(x, 1) = f'(1). \tag{4.7}_2$$

Substituting (4.4) into (4.6) results in the following conditions involving the coefficients, E_k and D_k:

$$\sum_{-\infty}^{\infty} \left[D_k \, e^{-2\hat{P}_k d/D} + E_k \right] \frac{\hat{\phi}_k(x)}{\hat{P}_k^2} = 0 \tag{4.8}$$

and

$$\sum_{-\infty}^{\infty} \left[D_k \, e^{-2\hat{P}_k d/D} + E_k \right] \hat{\phi}_k(x) + \sum_{-\infty}^{\infty} \left[D_k \, e^{-2\hat{P}_k d/D} \left(\frac{1 - \hat{P}_k}{\hat{P}_k} \right) - E_k \left(\frac{1 + \hat{P}_k}{\hat{P}_k} \right) \right] \hat{\phi}_k(x) = 0. \tag{4.9}$$

Next, substituting (4.5) into (4.7) gives the following conditions for the coefficients, A_k and B_k:

$$\sum_{-\infty}^{\infty} \left[A_k + B_k \right] \frac{\hat{\phi}_k(x)}{\hat{P}_k^2} = 0 \tag{4.10}$$

and

$$\sum_{-\infty}^{\infty} \left[A_k + B_k \right] \hat{\phi}_k(x) + \sum_{-\infty}^{\infty} \left[A_k \left(\frac{\coth \hat{P}_k - \hat{P}_k}{\hat{P}_k} \right) + B_k \left(\frac{\tanh \hat{P}_k - \hat{P}_k}{\hat{P}_k} \right) \right] \hat{\phi}_k(x) = 0. \tag{4.11}$$

5. Matching conditions

We shall require the continuity of velocities and stresses across common boundaries between each sub-region. It is not hard to show (see [25]) that the velocities and stresses will be continuous across the boundary between regions I and IV if

$$\Psi^{IV}\left(-\frac{W}{D}, y \right) = \Psi^{I}\left(-\frac{W}{D}, y \right),$$

$$\frac{\partial \Psi^{\mathrm{IV}}}{\partial x}\left(-\frac{W}{D}, y\right)=\frac{\partial \Psi^{\mathrm{I}}}{\partial x}\left(-\frac{W}{D}, y\right),$$
$$\frac{\partial^2 \Psi^{\mathrm{IV}}}{\partial x^2}\left(-\frac{W}{D}, y\right)=\frac{\partial^2 \Psi^{\mathrm{I}}}{\partial x^2}\left(-\frac{W}{D}, y\right),$$
$$\frac{\partial^3 \Psi^{\mathrm{IV}}}{\partial x^3}\left(-\frac{W}{D}, y\right)=\frac{\partial^3 \Psi^{\mathrm{I}}}{\partial x^3}\left(-\frac{W}{D}, y\right) \tag{5.1}$$

and the velocities and stresses will be continuous across the boundary between regions II and IV if

$$\Psi^{\mathrm{IV}}(x,-1)=\Psi^{\mathrm{II}}(x,-1),$$
$$\frac{\partial \Psi^{\mathrm{IV}}}{\partial y}(x,-1)=\frac{\partial \Psi^{\mathrm{II}}}{\partial y}(x,-1),$$
$$\frac{\partial^2 \Psi^{\mathrm{IV}}}{\partial y^2}(x,-1)=\frac{\partial^2 \Psi^{\mathrm{II}}}{\partial y^2}(x,-1),$$
$$\frac{\partial^3 \Psi^{\mathrm{IV}}}{\partial y^3}(x,-1)=\frac{\partial^3 \Psi^{\mathrm{II}}}{\partial y^3}(x,-1). \tag{5.2}$$

Substituting (4.4) and (4.5) into conditions $(5.1)_1$ leads us to the following relations among the coefficients of eigenfunctions in regions I and IV:

$$\sum_{-\infty}^{\infty}[C_k-Q_k]\frac{\phi_k(y)}{P_k^2}+\sum_{-\infty}^{\infty}[C_k^*-Q_k^*]\frac{\phi_k^*}{P_k^{*2}}=0, \tag{5.3}$$

$$\sum_{-\infty}^{\infty}P_k[C_k+Q_k\tanh P_kW/D]\frac{\phi_k(y)}{P_k^2}$$
$$+\sum_{-\infty}^{\infty}P_k^*[C_k^*+Q_k^*\tanh P_k^*W/D]\frac{\phi_k^*(y)}{P_k^{*2}}=0, \tag{5.4}$$

$$\sum_{-\infty}^{\infty}[C_k-Q_k]\phi_k(y)+\sum_{-\infty}^{\infty}[C_k^*-Q_k^*]\phi_k^*(y)$$
$$=\sum_{-\infty}^{\infty}\frac{B_k}{\hat{P}_k^2}\hat{\phi}_k''\left(\frac{W}{D}\right)\frac{\cosh\hat{P}_ky}{\cosh\hat{P}_k}+\sum_{-\infty}^{\infty}\frac{A_k}{\hat{P}_k^2}\hat{\phi}_k''\left(\frac{W}{D}\right)\frac{\sinh\hat{P}_ky}{\sinh\hat{P}_k}, \tag{5.5}$$

$$\sum_{-\infty}^{\infty}P_k\left[C_k+Q_k\tanh P_k\frac{W}{D}\right]\phi_k(y)$$
$$+\sum_{-\infty}^{\infty}P_k^*\left[C_k^*+Q_k^*\tanh P_k^*\frac{W}{D}\right]\phi_k^*(y)$$
$$=\sum_{-\infty}^{\infty}\frac{B_k}{\hat{P}_k^2}\hat{\phi}_k'''\left(\frac{W}{D}\right)\frac{\cosh\hat{P}_ky}{\cosh\hat{P}_k}-\sum_{-\infty}^{\infty}\frac{A_k}{\hat{P}_k^2}\hat{\phi}_k'''\left(\frac{W}{D}\right)\frac{\sinh\hat{P}_ky}{\sinh\hat{P}_k}. \tag{5.6}$$

Combining (4.4), (4.5) with (5.2), we get the following relations for the coefficients of the eigenfunctions in regions II and IV:

$$\sum_{-\infty}^{\infty}\left[D_k+E_k\,\mathrm{e}^{-2\hat{P}_k d/D}+A_k-B_k\right]\frac{\hat{\phi}_k(x)}{\hat{P}_k^2}=f(-1), \tag{5.7}$$

$$\sum_{-\infty}^{\infty}\hat{P}_k\left[D_k-E_k\,\mathrm{e}^{-2\hat{P}_k d/D}-A_k\coth\hat{P}_k+B_k\tanh\hat{P}_k\right]\frac{\hat{\phi}_k(x)}{\hat{P}_k^2}=f'(-1), \tag{5.8}$$

$$\begin{aligned}\sum_{-\infty}^{\infty}\left[D_k+E_k\,\mathrm{e}^{-2\hat{P}_k d/D}+A_k-B_k\right]\hat{\phi}_k(x)&=f''(-1)\\ &+\sum_{-\infty}^{\infty}Q_k\frac{\phi_k''(1)}{P_k^2}\frac{\cosh P_k x}{\cosh P_k W/D}-\sum_{-\infty}^{\infty}Q_k^*\frac{\phi_k^{*\prime\prime}(1)}{P_k^{*2}}\frac{\cosh P_k^* x}{\cosh P_k^* W/D},\end{aligned} \tag{5.9}$$

$$\begin{aligned}\sum_{-\infty}^{\infty}\hat{P}_k\left[D_k-E_k\,\mathrm{e}^{-2\hat{P}_k d/D}-A_k\coth P_k+B_k\tanh P_k\right]\hat{\phi}_k(x)&=f'''(-1)\\ &-\sum_{-\infty}^{\infty}Q_k\frac{\phi_k'''(1)}{P_k^2}\frac{\cosh P_k x}{\cosh P_k W/D}+\sum_{-\infty}^{\infty}Q_k^*\frac{\hat{\phi}_k'''(1)}{P_k^{*2}}\frac{\cosh P_k^* x}{\cosh P_k^* W/D}.\end{aligned} \tag{5.10}$$

6. Biorthogonality—determination of the coefficients

The eqns. (4.8) through (4.11) and (5.3) through (5.10) are now expressed in a form which will facilitate the implementation of biorthogonality. First we define

$$\phi_1^k(s)=\phi_k(s),\qquad \phi_2^k(s)=\phi_k''(s)/P_k^2;$$
$$\hat{\phi}_1^k(s)=\hat{\phi}_k(s),\qquad \hat{\phi}_2^k(s)=\hat{\phi}_k''(s)/\hat{P}_k^2$$

and

$$\phi_1^{*k}(s)=\phi_k^*(s),\qquad \phi_2^{*k}(s)=\phi_k^{*\prime\prime}(s)/P_k^{*2}.$$

The vector form of eqns. (4.8)–(4.11) and (5.3)–(5.10) is

$$\begin{aligned}\sum_{-\infty}^{\infty}\left[D_k\,\mathrm{e}^{-2\hat{P}_k d/D}+E_k\right]\begin{bmatrix}\hat{\phi}_1^k(x)\\ \hat{\phi}_2^k(x)\end{bmatrix}&\\ +\sum_{-\infty}^{\infty}\left[D_k\,\mathrm{e}^{-2\hat{P}_k d/D}\left(\frac{1-\hat{P}_k}{\hat{P}_k}\right)-E_k\left(\frac{1+\hat{P}_k}{\hat{P}_k}\right)\right]\begin{bmatrix}\hat{\phi}_1^k(x)\\ 0\end{bmatrix}&=\begin{bmatrix}0\\0\end{bmatrix},\end{aligned} \tag{6.1}$$

$$\begin{aligned}\sum_{-\infty}^{\infty}\left[A_k+B_k\right]\begin{bmatrix}\hat{\phi}_1^k(x)\\ \hat{\phi}_2^k(x)\end{bmatrix}&\\ +\sum_{-\infty}^{\infty}\left[A_k\left(\frac{\coth\hat{P}_k-\hat{P}_k}{\hat{P}_k}\right)+B_k\left(\frac{\tanh\hat{P}_k-\hat{P}_k}{\hat{P}_k}\right)\right]\begin{bmatrix}\hat{\phi}_1^k(x)\\ 0\end{bmatrix}&=\begin{bmatrix}0\\0\end{bmatrix},\end{aligned} \tag{6.2}$$

$$\sum_{-\infty}^{\infty}[C_k - Q_k]\begin{bmatrix}\phi_1^k(y)\\ \phi_2^k(y)\end{bmatrix} + \sum_{-\infty}^{\infty}[C_k^* - Q_k^*]\begin{bmatrix}\phi_1^*(y)\\ \phi_2^*(y)\end{bmatrix}$$

$$= \begin{bmatrix}\sum_{-\infty}^{\infty} B_k \dfrac{\hat{\phi}_k''(W/D)}{\hat{P}_k^2}\dfrac{\cosh \hat{P}_k y}{\cosh \hat{P}_k}\\ 0\end{bmatrix} + \begin{bmatrix}\sum_{-\infty}^{\infty} A_k \dfrac{\hat{\phi}_k''(W/D)}{\hat{P}_k^2}\dfrac{\sinh \hat{P}_k y}{\sinh \hat{P}_k}\\ 0\end{bmatrix} \tag{6.3}$$

$$\sum_{-\infty}^{\infty} P_k[C_k + Q_k \tanh P_k W/D]\begin{bmatrix}\phi_1^k(y)\\ \phi_2^k(y)\end{bmatrix}$$

$$+ \sum_{-\infty}^{\infty} P_k^*[C_k^* + Q_k^* \tanh P_k^* W/D]\begin{bmatrix}\phi_1^{*k}(y)\\ \phi_2^{*k}(y)\end{bmatrix}$$

$$= -\begin{bmatrix}\sum_{-\infty}^{\infty} B_k \dfrac{\hat{\phi}_k'''(W/D)}{\hat{P}_k^2}\dfrac{\cosh \hat{P}_k y}{\cosh \hat{P}_k}\\ 0\end{bmatrix} - \begin{bmatrix}\sum_{-\infty}^{\infty} A_k \dfrac{\hat{\phi}_k'''(W/D)}{\hat{P}_k^2}\dfrac{\sinh \hat{P}_k y}{\sinh \hat{P}_k}\\ 0\end{bmatrix} \tag{6.4}$$

$$\sum_{-\infty}^{\infty}\left[D_k + E_k\, e^{-2\hat{P}_k d/D} + A_k - B_k\right]\begin{bmatrix}\hat{\phi}_1^k(x)\\ \hat{\phi}_2^k(x)\end{bmatrix}$$

$$= \begin{bmatrix} f''(-1) + \sum_{-\infty}^{\infty} Q_k \dfrac{\phi_k''(1)}{P_k^2}\dfrac{\cosh P_k x}{\cosh P_k W/D} - \sum_{-\infty}^{\infty} Q_k^* \dfrac{\phi_k^{*\prime\prime}(1)}{P_k^{*2}}\dfrac{\cosh P_k^* x}{\cosh P_k^* W/D}\\ 0\end{bmatrix}, \tag{6.5}$$

$$\sum_{-\infty}^{\infty}\hat{P}_k\left[D_k - E_k\, e^{-2\hat{P}_k d/D} + A_k \coth \hat{P}_k + B_k \tanh \hat{P}_k\right]\begin{bmatrix}\hat{\phi}_1^k(x)\\ \hat{\phi}_2^k(x)\end{bmatrix}$$

$$= \begin{bmatrix} f'''(-1) - \sum_{-\infty}^{\infty} Q_k \dfrac{\phi_k'''(1)}{P_k^2}\dfrac{\cosh P_k x}{\cosh P_k W/D} + \sum_{-\infty}^{\infty} Q_k^* \dfrac{\phi_k^{*\prime\prime\prime}(1)}{P_k^{*2}}\dfrac{\cosh P_k^* x}{\cosh P_k^* W/D}\\ 0\end{bmatrix} \tag{6.6}$$

To obtain the above expressions we twice differentiated eqns. (4.8), (4.10), (5.3), (5.4), (5.7) and (5.8).

The biorthogonality properties for the eigenfunctions appearing in eqns. (6.1)–(6.6) are summarized below:

$$\int_{-1}^{1} \boldsymbol{A}\boldsymbol{\phi}^k(s)\cdot\boldsymbol{\psi}^n(s)\,\mathrm{d}s = k_n\delta_{nk},$$

$$\int_{-1}^{1} \boldsymbol{A}\boldsymbol{\phi}^{*k}(s) \cdot \boldsymbol{\psi}^{*n}(s)\, \mathrm{d}s = k_n^* \delta_{nk},$$

$$\int_{-W/D}^{W/D} \boldsymbol{A}\hat{\boldsymbol{\phi}}^{k}(s) \cdot \hat{\boldsymbol{\psi}}^{n}(s)\, \mathrm{d}s = \frac{W}{D} k_n \delta_{nk},$$

where

$$A_{ij} = \begin{bmatrix} 0 & -1 \\ 1 & 2 \end{bmatrix},$$

$$k_n = -4 \cos^4 P_n,$$

$$k_n^* = -4 \sin^4 P_n^*,$$

$$\phi_i^k(s) = \begin{bmatrix} \phi_1^k(s) \\ \phi_2^k(s) \end{bmatrix}$$

and $\boldsymbol{\psi}^n(s)$ and $\boldsymbol{\psi}^{*n}(s)$ are, respectively, the vectors containing the even and odd adjoint eigenfunctions. The adjoint eigenfunctions are given by Joseph and Sturges [16] as

$$\psi_1^n(s) = \phi_1^n(s) - 2 \cos P_n \cos P_n s \equiv \psi_n(s),$$

$$\psi_2^n(s) = -\frac{\psi_n''(s)}{P_n^2} = \phi_1^n(s),$$

$$\psi_1^{*n}(s) = \phi_1^{*n}(s) + 2 \sin P_n^* \sin P_n^* s \equiv \psi_n^*(s)$$

and

$$\psi_2^{*n}(s) = -\frac{\psi_n^{*\prime\prime}(s)}{P_n^{*2}} = \phi_1^{*n}(s).$$

The adjoint eigenfunctions, $\hat{\boldsymbol{\psi}}^n(s)$, bear the same relationship to $\hat{\boldsymbol{\phi}}^n(s)$ as $\boldsymbol{\psi}^n(s)$ does to $\boldsymbol{\phi}^n(s)$. To implement biorthogonality we use the operators defined below:

$$\begin{aligned} &\int_{-1}^{1} \boldsymbol{A}(\circ) \cdot \boldsymbol{\psi}^n(s)\, \mathrm{d}s, \\ &\int_{-1}^{1} \boldsymbol{A}(\circ) \cdot \boldsymbol{\psi}^{*n}(s)\, \mathrm{d}s, \\ &\int_{-W/D}^{W/D} \boldsymbol{A}(\circ) \cdot \hat{\boldsymbol{\psi}}^n(s)\, \mathrm{d}s. \end{aligned} \tag{6.7}$$

The operator $(6.7)_3$ is first applied to eqns. (6.1), (6.2), (6.5) and (6.6). This

leads to

$$D_n e^{-2\hat{P}_n d/D} + E_n + \sum_{-\infty}^{\infty} D_k e^{-2\hat{P}_k d/D}\left(\frac{1-\hat{P}_k}{\hat{P}_k}\right)\frac{\hat{G}_{nk}}{k_n} - \sum_{-\infty}^{\infty} E_k\left(\frac{1+\hat{P}_k}{\hat{P}_k}\right)\frac{\hat{G}_{nk}}{k_n} = 0, \tag{6.9}$$

$$A_n + B_n + \sum_{-\infty}^{\infty} A_k\left(\frac{\coth \hat{P}_k - \hat{P}_k}{\hat{P}_k}\right)\frac{\hat{G}_{nk}}{k_n} + \sum_{-\infty}^{\infty} B_k\left(\frac{\tanh \hat{P}_k - \hat{P}_k}{\hat{P}_k}\right)\frac{\hat{G}_{nk}}{k_n} = 0, \tag{6.10}$$

$$D_n + E_n e^{-2\hat{P}_n d/D} + A_n - B_n = \frac{4}{k_n} f''(-1) + \sum_{-\infty}^{\infty} Q_k \frac{\phi_k''(1)}{P_k^2}\frac{\Lambda(P_n, P_k W/D)}{k_n \cosh P_k W/D} - \sum_{-\infty}^{\infty} Q_k^* \frac{\phi_k^{*\prime\prime}(1)}{P_k^{*2}}\frac{\Lambda(P_n, P_k^* W/D)}{k_n \cosh P_k^* W/D}, \tag{6.11}$$

$$D_n - E_n e^{-2\hat{P}_n d/D} - A_n \coth \hat{P}_n + B_n \tanh \hat{P}_n = \frac{4}{k_n \hat{P}_n} f'''(-1) + \sum_{-\infty}^{\infty} Q_k \frac{\phi_k'''(1)}{P_k^2}\frac{\Lambda(P_n, P_k W/D)}{k_n \cosh P_k W/D} + \sum_{\infty}^{\infty} Q_k^* \frac{\phi_k^{*\prime\prime\prime}(1)}{P_k^{*2}}\frac{\Lambda(P_n, P_k^* W/D)}{k_n \cosh P_k^* W/D}. \tag{6.12}$$

where

$$4 = \frac{1}{W/D}\int_{-W/D}^{W/D} \hat{\psi}_2^n(x)\, dx,$$

$$\hat{G}_{nk} = \frac{1}{W/D}\int_{-W/D}^{W/D} \hat{\psi}_2^n(x)\phi_1^k(x)\, dx,$$

$$\Lambda(P_n, P_k W/D) = \frac{1}{W/D}\int_{-W/D}^{W/D} \cosh P_k x \hat{\psi}_2^n(x)\, dx$$

and $\Lambda(P_n, P_k^* W/D)$ is obtained from $\Lambda(P_n, P_k W/D)$ by placing an asterisk (*) on the sub-scripted "k" quantities. Next, the operators (6.7), and $(6.7)_2$ are applied to eqns. (6.3) and (6.4). This leads to

$$C_n - Q_n = \sum_{-\infty}^{\infty} B_k \frac{\hat{\phi}_k''(W/D)}{\hat{P}_k^2}\frac{\Lambda(P_n, \hat{P}_k)}{k_n \cosh \hat{P}_k}, \tag{6.13}$$

$$C_n^* - Q_n^* = \sum_{-\infty}^{\infty} A_k \frac{\hat{\phi}_k''(W/D)}{\hat{P}_k^2}\frac{\Lambda^*(P_n^*, \hat{P}_k)}{k_n^* \sinh \hat{P}_k}, \tag{6.14}$$

$$C_n + Q_n \tanh P_n W/D = -\sum_{-\infty}^{\infty} B_k \frac{\hat{\phi}_k'''(W/D)}{\hat{P}_k^2} \frac{\Lambda(P_n, \hat{P}_k)}{P_n k_n \cosh \hat{P}_k}, \tag{6.15}$$

$$C_n^* + Q_n^* \tanh P_n^* W/D = -\sum_{-\infty}^{\infty} A_k \frac{\hat{\phi}_k'''(W/D)}{\hat{P}_k^2} \frac{\Lambda^*(P_n^*, \hat{P}_k)}{P_n^* k_n^* \sinh \hat{P}_k}, \tag{6.16}$$

where

$$\Lambda(P_n, \hat{P}_k) = \int_{-1}^{1} \cosh \hat{P}_k y \psi_2^n(y)\, \mathrm{d}y$$

and

$$\Lambda^*(P_n^*, \hat{P}_k) = \int_{-1}^{1} \sinh \hat{P}_k y \psi_2^{*n}(y)\, \mathrm{d}y.$$

Equations (6.13)–(6.16) may be solved for the coefficients C_n, C_n^*, Q_n and Q_n^* in terms of the coefficients A_k and B_k. Symbolically, we find that

$$C_n = -\sum_{-\infty}^{\infty} {}^1R_{nk} B_k, \tag{6.17}$$

$$Q_n = -\sum_{-\infty}^{\infty} {}^2R_{nk} B_k, \tag{6.18}$$

$$C_n^* = \sum_{-\infty}^{\infty} {}^3R_{nk} A_k, \tag{6.19}$$

and

$$Q_n^* = \sum_{-\infty}^{\infty} {}^4R_{nk} A_k. \tag{6.20}$$

Equations (6.11) and (6.12) may now be solved for the coefficients D_n and E_n in terms of the coefficients A_k and B_k by using the expressions for Q_n and Q_n^* given in eqns. (6.18) and (6.20). Thus,

$$D_n = \tfrac{1}{2}\left[{}^1g_n + {}^1H_{nk} B_k - {}^2H_{nk} A_k\right] \tag{6.21}$$

and

$$E_n\, \mathrm{e}^{-2\hat{P}_n d/D} = \tfrac{1}{2}\left[{}^2g_n - {}^3H_{nk} B_k + {}^4H_{nk} A_k\right], \tag{6.22}$$

where

$${}^1H_{nk} = {}^5R_{nm}\, {}^2R_{mk} + (1 - \tanh \hat{P}_n)\, \delta_{nk},$$

$${}^2H_{nk} = {}^6R_{nm}\, {}^4R_{mk} + (1 - \coth \hat{P}_n)\, \delta_{nk},$$

$${}^3H_{nk} = {}^7R_{nm}\, {}^2R_{mk} - (1 + \tanh \hat{P}_n)\, \delta_{nk},$$

$${}^4H_{nk} = {}^8R_{nm}\, {}^4R_{mk} - (1 + \coth \hat{P}_n)\, \delta_{nk},$$

$$ {}^{1}g_n = \frac{4}{k_n}\left[f''(-1) + \frac{f'''(-1)}{\hat{P}_n} \right], $$

$$ {}^{2}g_n = \frac{4}{k_n}\left[f''(-1) - \frac{f'''(-1)}{\hat{P}_n} \right] $$

and δ_{nk} is the Kronecker delta. The reader is referred to Trogdon [26] for explicit representation of the quantities ${}^{1}R_{ij}$ through ${}^{8}R_{ij}$. In the above expressions and in what follows the summation signs have been dropped and a repeated index implies summation with respect to that index. From eqn. (6.10), the coefficients A_n may be found in terms of the coefficients B_k. Thus

$$ A_n = -({}^{1}G^{-1})_{nj}\,{}^{2}G_{jk}B_k, \tag{6.23} $$

where

$$ {}^{1}G_{nk} = \left(\frac{\coth \hat{P}_k - \hat{P}_k}{\hat{P}_k} \right) \frac{\hat{G}_{nk}}{k_n} + \delta_{nk} $$

and

$$ {}^{2}G_{nk} = \left(\frac{\tanh \hat{P}_k - \hat{P}_k}{\hat{P}_k} \right) \frac{\hat{G}_{nk}}{k_n} + \delta_{nk}. $$

Equation (6.9) may be solved for the coefficients E_n, yielding

$$ E_n \, \mathrm{e}^{-2\hat{P}_n d/D} = \hat{H}_{nk} D_k, \tag{6.24} $$

where

$$ \hat{H}_{nk} = \mathrm{e}^{-2\hat{P}_n d/D}({}^{4}G^{-1})_{nj}\,{}^{3}G_{jk}\,\mathrm{e}^{-2\hat{P}_k d/D}, $$

$$ {}^{3}G_{nk} = \left(\frac{1 - \hat{P}_k}{\hat{P}_k} \right) \frac{\hat{G}_{nk}}{k_n} + \delta_{nk}, $$

and

$$ {}^{4}G_{nk} = \left(\frac{1 + \hat{P}_k}{\hat{P}_k} \right) \frac{\hat{G}_{nk}}{k_n} - \delta_{nk}. $$

Substituting eqns. (6.21) and (6.22) into (6.24), using (6.23), results in the following system of equations for the coefficients B_k,

$$ \left\{ {}^{2}H_{ni}({}^{1}G^{-1})_{ij}\,{}^{2}G_{jk} + {}^{3}H_{nk} + \hat{H}_{nm}\left[{}^{2}H_{mi}({}^{1}G^{-1})_{ij}\,{}^{2}G_{jk} + {}^{1}H_{mk} \right] \right\} B_k $$
$$ = {}^{2}g_n - \hat{H}_{nm}\,{}^{1}g_m. \tag{6.25} $$

Once the B_k are determined the other coefficients may be determined by

matrix multiplication and addition. The form of eqns. (6.25) is particularly interesting. All matrices appearing depend on the parameter W/D, except $\hat{\boldsymbol{H}}$ which depends upon the parameter d/D. Therefore the system of equations (6.25) is particularly convenient for parametric studies where W/D is fixed and d/D is varied.

The system of equations (6.25) is an infinite system of equations. This system is solved by truncation. The result is a determination of the coefficients, $B_k^{(N)}$, $A_k^{(N)}$, $E_k^{(N)}$, $D_k^{(N)}$, $C^{*(N)}_k$, $C_k^{(N)}$, $Q_k^{(N)}$ and $Q^{*(N)}_k$ which are approximations to the actual coefficients under truncation.

To compute the right hand side of (6.25) one must know $f(y) = \lim_{x\to\pm\infty}\Psi(x,y)$. It is easy to show that nondimensionalizing the stream function by the flow rate in the channel implies that

$$\Psi(x,y) \to \tfrac{1}{4}(y+1)^2 \quad \text{as } x \to \pm\infty$$

for the shear (top plate) driven flow, and

$$\Psi(x,y) \to y(3-y^2)/4 + \tfrac{1}{2} \quad \text{as } x \to \pm\infty$$

for the pressure driven flow.

7. Evaluation of the Newtonian pressure

The Newtonian pressure is found as a solution of

$$\operatorname{grad}\Phi_0 = \nabla^2 \boldsymbol{u},$$

where

$$\Phi_0 = \frac{\hat{\Phi}_0}{4\mu Q/D^2}.$$

Thus, in region I

$$\Phi_0^{\mathrm{I}} = f'''(y)x + 2\sum_{-\infty}^{\infty} C_n \cos P_n \sin(P_n y)\, e^{P_n(x+W/D)} + 2\sum_{-\infty}^{\infty} C_n^* \sin P_n^* \cos(P_n^* y)\, e^{P_n^*(x+W/D)} + C^{\mathrm{I}};$$

in region II

$$\Phi_0^{\mathrm{II}} = -2\sum_{-\infty}^{\infty} D_n \cos P_n \sin\left(P_n \frac{x}{W/D}\right) e^{\hat{P}_n(y+1)} + 2\sum_{-\infty}^{\infty} E_n \cos P_n \sin\left(P_n \frac{x}{W/D}\right) e^{-\hat{P}_n(y+1+2d/D)} + C^{\mathrm{II}};$$

and in region IV

$$\Phi_0^{IV} = f'''(y)x \quad +2\sum_{-\infty}^{\infty} Q_n \cos P_n \sin P_n y \frac{\sinh P_n x}{\cosh P_n W/D}$$
$$+2\sum_{-\infty}^{\infty} Q_n^* \cos P_n^* y \frac{\sinh P_n^* x}{\cosh P_n^* W/D}$$
$$-2\sum_{-\infty}^{\infty} A_n \cos P_n \sin P_n \frac{x}{W/D} \frac{\cosh \hat{P}_n y}{\sinh \hat{P}_n}$$
$$-2\sum_{-\infty}^{\infty} B_n \cos P_n \sin P_n \frac{x}{W/D} \frac{\sinh \hat{P}_n y}{\cosh \hat{P}_n}$$
$$+C^{IV},$$

where C^I, C^{II} and C^{IV} are constants. These constants may be determined by matching the pressures along their common boundaries. It is easy to show that $C^{II} = C^{IV}$ and evaluating

$$\int_{-1}^{1} \left(\Phi_0^I - \Phi_0^{IV}\right)|_{x=-W/D}\, dy = 0$$

gives

$$C^I - C^{IV} = \sum_{-\infty}^{\infty} \frac{Q_n^*}{P_n^*} \sin^2 P_n^* \tanh P_n^* \frac{W}{D} - \frac{W}{D} \sum_{-\infty}^{\infty} A_n - \sum_{\infty}^{\infty} \frac{C_n^*}{P_n^*} \sin^2 P_n^*.$$

8. Results and discussion

Streamline plots for the shear driven and pressure driven flows are given in Figs. 4–9. Figures 4–6 are for the shear (top plate) driven flow. The ratio $W/D = 1$ is fixed and the ratio d/D is varied. The flow in Fig. 4 is

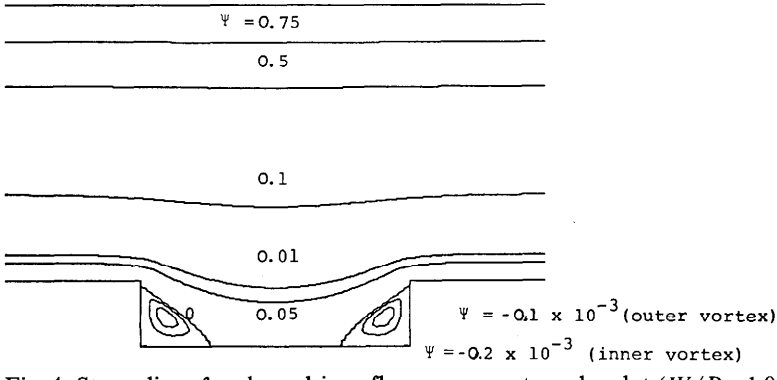

Fig. 4. Streamlines for shear driven flow over a rectangular slot ($W/D = 1.0$, $d/D = 0.24$).

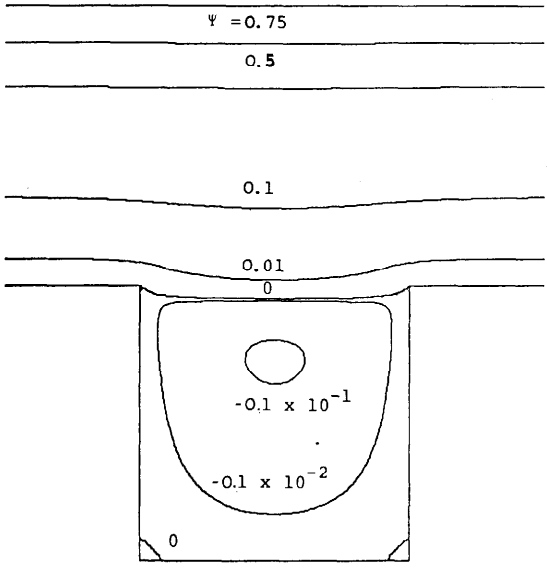

Fig. 5. Streamlines for shear driven flow over a rectangular slot ($W/D=1.0$, $d/D=1.0$).

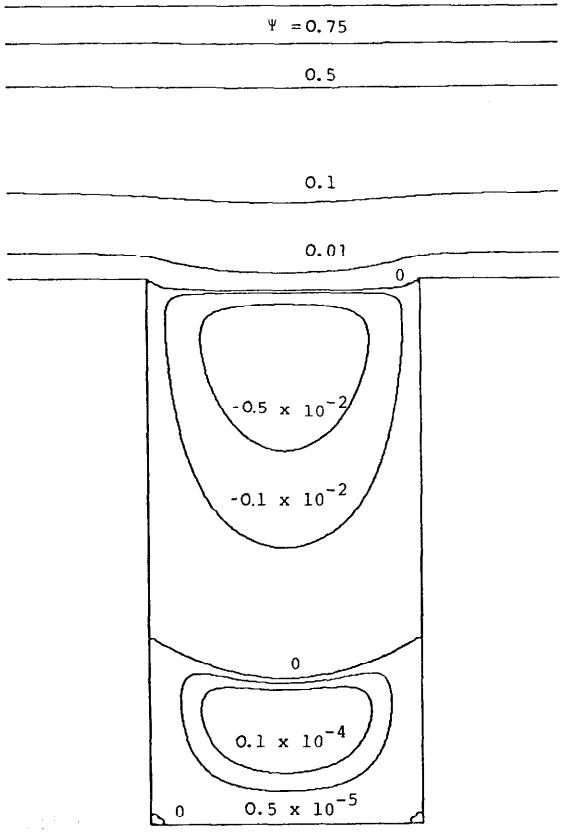

Fig. 6. Streamlines for shear driven flow over a rectangular slot ($W/D=1.0$, $d/D=2.0$).

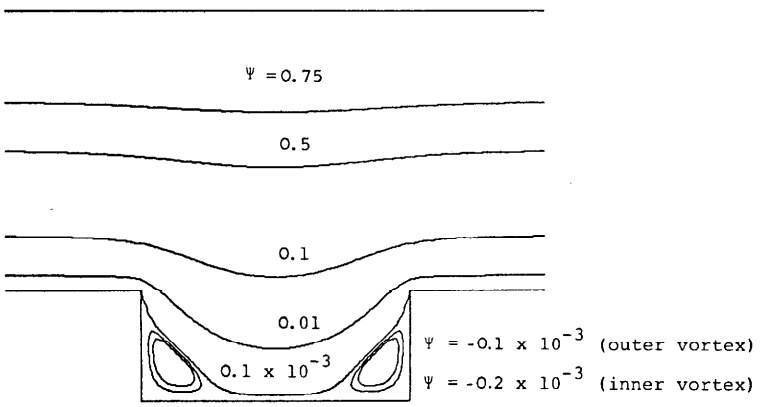

Fig. 7. Streamlines for pressure driven flow over a rectangular slot ($W/D=1.0$, $d/D=0.5$).

dominated by corner eddies. As d/D is increased the corner eddies coalesce to form one central eddy as shown in Fig. 4. A further increase in d/D results again in the coalescence of corner eddies yielding two central eddies (see Fig. 6). The same sequence of eddies is shown in Figs. 7–9 for the pressure driven case. One interesting difference between the two flows is the depth the channel flow penetrates the slot. The pressure driven flow always penetrates further into the slot.

The hole pressure P_e, given by (2.2) for the pressure driven flow, is shown in Fig. 10. For the values $W/D=0.5$ and $W/D=1.0$, P_e is essentially

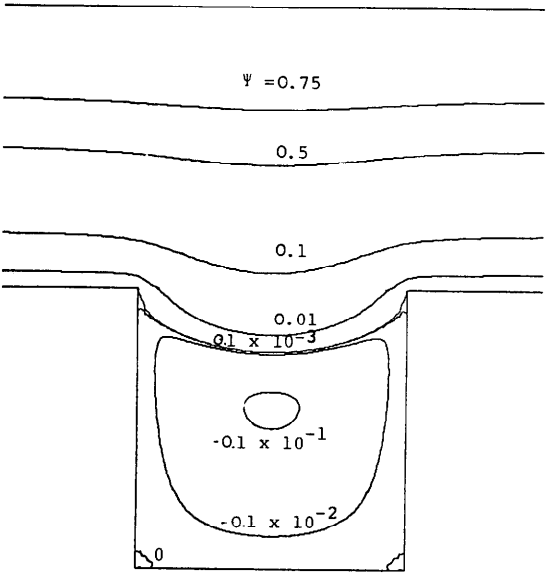

Fig. 8. Streamlines for pressure driven flow over a rectangular slot ($W/D=1.0$, $d/D=1.0$).

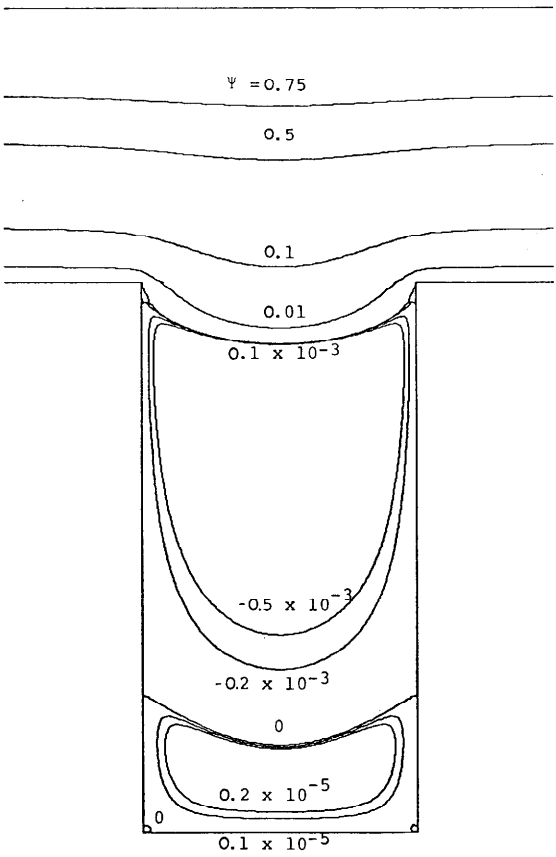

Fig. 9. Streamlines for pressure driven flow over a rectangular slot ($W/D=1.0$, $d/D=2.0$).

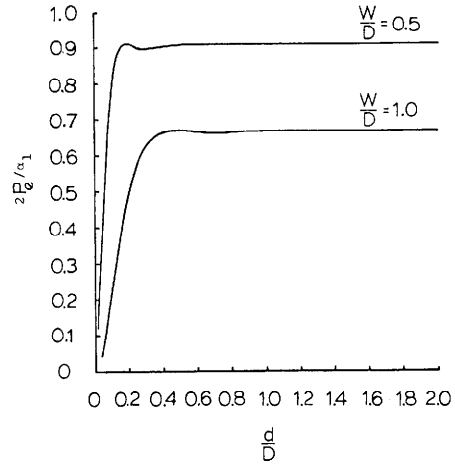

Fig. 10. Variation of the hole pressure (pressure driven flow) with d/D for $W/D=0.5$ and 1.0.

independent of slot depth d whenever $d/D > 0.5W/D$. P_e depends significantly on the dimensions of the slot and it increases, for fixed W/D, as d/D increases. Our numerical technique for computing P_e does not work well as the depth-width ratio d/W tends to zero for fixed values of W/D.

To determine P_e from experiments one usually positions two force transducers opposite each other and symmetrically located about the centerline of the slot. The difference between the output of the two transducers gives a measure of P_e. Using (2.1) we evaluate $\hat{T}\langle yy\rangle$ on a stationary boundary as

$$\hat{T}\langle yy\rangle = -\hat{\Phi}_0 + \frac{\alpha_1}{2}\left(\frac{\partial \hat{u}}{\partial \hat{y}}\right)^2.$$

The quantities used to determine the difference between the force on the top of the slot and the bottom of the slot are the Newtonian pressure and the velocity gradient. In Fig. 11 the Newtonian pressure discrepancy

$$\Phi_0^{\mathrm{IV}}(x, 1) - \Phi_0^{\mathrm{II}}(x, -1 - 2d/D)$$

is exhibited and the normal stress discrepancy

$$\frac{\left(\dfrac{\partial u^{\mathrm{IV}}}{\partial y}(x, 1)\right)^2 - \left(\dfrac{\partial u^{\mathrm{II}}}{\partial y}(x, -1 - 2d/D)\right)^2}{\lim\limits_{x \to \pm\infty}\left(\dfrac{\partial u}{\partial y}\right)^2\Big|_{y=\pm 1}}$$

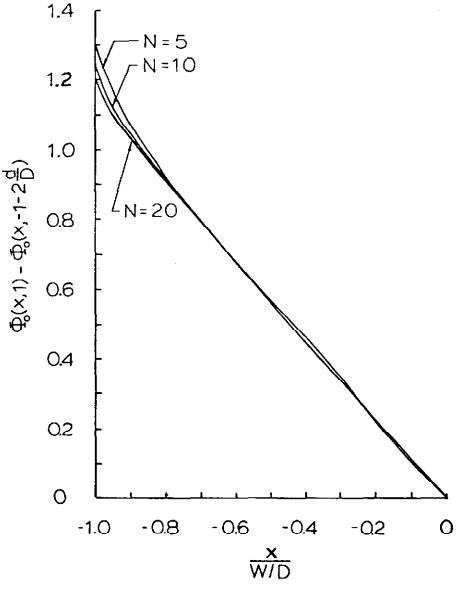

Fig. 11. The Newtonian pressure discrepancy for different truncation numbers (pressure driven flow with $W/D = 1.0$, $d/D = 1.0$).

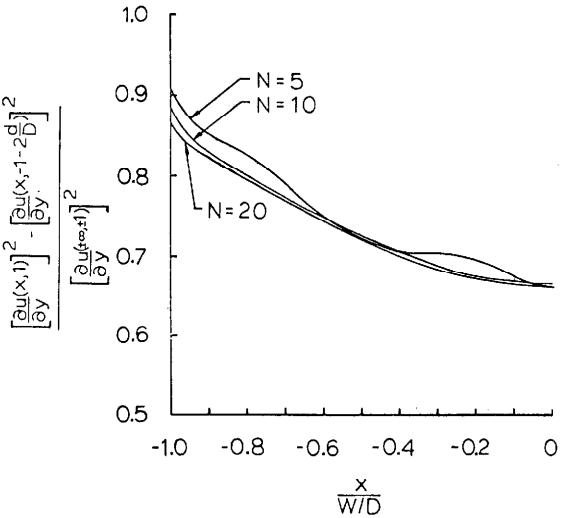

Fig. 12. The normal stress discrepancy for different truncation numbers (pressure driven flow with $W/D = 1.0$, $d/D = 1.0$).

is shown in Fig. 12. Both distributions are shown for $W/D = 1.0$, $d/D = 1.0$ and truncation numbers $N = 5$, 10 and 20.

For $N = 5$ oscillations are apparent. For $N = 10$ the oscillations have been smoothed out; there is almost no change in the graphs as N is increased from 10 to 20. For practical purposes it would appear that a truncation number of $N = 20$ is sufficient. The streamline plots given in this section were all generated using a truncation number of $N = 10$.

Our streamline plots are directly comparable with those given by O'Brien [9]. The agreement is quite good but our results appear to be more accurate in that with relatively few eigenfunctions we can predict details of flow such as corner eddies. O'Brien is mainly concerned with predicting streamline patterns and thus makes no calculation of the hole pressure. Malkus [11] was probably the first to use numerical methods to compute the hole pressure for the Stokes flow. Again, our results appear to be more accurate in that we do predict a reversal in P_e as the slot depth is increased. This reversal becomes less apparent with increasing slot width. The reversal in P_e is consistent with the vortex structure of the flow in the slot. The depth at which reversal first occurs is a strong function of the slot width (see Fig. 10). Malkus gives no indication of the accuracy of his results, while we have shown for the slot $W/D = 1$, $d/D = 1$ that our method of computing P_e appears to give accurate results when relatively few eigenfunctions are used. Mir-Mohamad-Sadegh and Rajagopal [12] give details of how to solve the same Stokes flow problem using a boundary integral technique. They state that the hole

pressure can be computed using their solution but they make no attempt to compute it. Townsend [10] notes that inertia is an important parameter in flow over a slot. Either the inertial contribution to the flow must be known or else its effects must be minimized if the Stokes solution is to be used to compute the hole pressure. We have shown in § 2 when the Stokes approximation is valid and thus when elastic effects will dominate the flow at second order. In Fig. 10 we have shown the extent to which elastic effects depend on the geometry of the slot.

Appendix: Shear driven motions perturbing rest in a deep cavity

In our study we have used the half-depth $D/2$ of the channel as the unit of length. This choice is restrictive since it rules out the problem in which $D \to 0$ and the fluid at the top of the slot is driven by the shearing of a scraping plate which is dragged across the slot with a uniform velocity U. This limiting problem has been solved with biorthogonal series by Joseph and Sturges [16]. They showed that the influence of the data on the edge (U in this case) has essentially decayed to zero in a distance $2W$. In the slot interior a few gap widths away from the end the solution is dominated by one eigenfunction which may be described as decaying oscillation of fixed period. For the semi-infinite slot ($d \to \infty$) with even data the interior form of the stream function is given by

$$\Psi(x,y) \simeq a_1\phi_1(x)\, e^{P_1 y} + \text{complex conjugate}, \tag{A.1}$$

where $\phi_1(x)$ is defined under (4.2) and

$$P_1 = 2.106196 + i\ 1.125365. \tag{A.2}$$

In problems in which general data are prescribed at the top of the slot the interior form of the stream function is a linear combination of the leading eigenfunctions of even and odd parity

$$\Psi(x,y) \simeq a_1\phi_1(x)\, e^{P_1 y} + a_2\hat{\phi}_1(x)\, e^{\hat{P}_1 y} + \text{complex conjugate}, \tag{A.3}$$

where $\phi_1(x)$ and P_1 are given by (A.1) and (A.2) and $\hat{\phi}_1(x) = \hat{\phi}_1^{(1)}(x)$ is the odd eigenfunction defined by $(A.5)_4$ and $\hat{P}_1 = \hat{p}_1$ is the first root of $(A.5)_5$.

There is a sense in which the expression (A.3) is the universal form for *all* steady solutions not only of the Navier–Stokes equations but also for any fluid whose constitutive equation collapses to a Newtonian one in slow steady flow. The reason is that no matter how violent the steady motion at the top of the slot may be, the solution deep in the slot is dominated by stationary walls and is slow and steady.

We close our discussion of biorthogonal series solutions of slot problems with an analysis of the hole pressure in a deep slot when the shear stress

$\tau(x,0)$ at the top of the slot is prescribed. For mathematical convenience we shall suppose that the top edge of the slot is a streamline, $\Psi(x,0)=0$.

The Stokes flow problem corresponding to this slot configuration is governed by the biharmonic equation

$$\nabla^4\Psi=0 \quad \text{in } -1\leqslant x\leqslant 1, y<0, \tag{A.4}$$

with boundary conditions

$$\Psi(x,0)=0,$$

$$\Psi_{yy}(x,0)=f(x),$$

$$\Psi(x,-\infty)=0,$$

$$\Psi(\pm 1,y)=0,$$

$$\Psi_x(\pm 1,y)=0.$$

This problem has an exact solution in biorthogonal series

$$\Psi(x,y)=\sum_{-\infty}^{\infty} C_n\phi_1^{(n)}(x)\,e^{P_n y}+\sum_{-\infty}^{\infty}\hat{C}_n\hat{\phi}_1^{(n)}(x)\,e^{\hat{p}_n y}$$

$$\phi_1^{(n)}(x)=p_n\sin p_n\cos p_n x-p_n x\cos p_n\sin p_n x$$

$$\sin 2p_n+2p_n=0,$$

$$\hat{\phi}_1^{(n)}(x)=\hat{p}_n\cos\hat{p}_n\sin\hat{p}_n x-\hat{p}_n x\sin\hat{p}_n\cos\hat{p}_n x$$

$$\sin 2\hat{p}_n-2\hat{p}_n=0. \tag{A.5}$$

The coefficients in the series $(A.5)_1$ are given by

$$C_n=\frac{1}{k_n}\int_{-1}^{1}\left[\psi_1^{(n)}(x),\psi_2^{(n)}(x)\right]\begin{bmatrix}0 & -1\\ 1 & 2\end{bmatrix}\begin{bmatrix}f(x)\\ 0\end{bmatrix}dx,$$

$$k_n=-4\cos^4 p_n$$

and

$$\hat{C}_n=\frac{1}{\hat{k}_n}\int_{-1}^{1}\left[\hat{\psi}_1^{(n)}(x),\hat{\psi}_2^{(n)}(x)\right]\begin{bmatrix}0 & -1\\ 1 & 2\end{bmatrix}\begin{bmatrix}f(x)\\ 0\end{bmatrix}dx$$

$$\hat{k}_n=-4\sin^4\hat{p}_n,$$

where

$$\psi_2^{(n)}(x)=\phi_1^{(n)}(x),$$

$$\hat{\psi}_2^{(n)}(x)=\hat{\phi}_1^{(n)}(x),$$

$$\psi_1^{(n)}(x)=\phi_1^{(n)}(x)-2\cos p_n\cos p_n x,$$

$$\hat{\psi}_1^{(n)}(x)=\hat{\phi}_1^{(n)}(x)+2\sin\hat{p}_n\sin\hat{p}_n x$$

are adjoint eigenfunctions.

If $\tau(x,0)$ is even in x, $\hat{C}_n = 0$; if it is odd in x, then $C_n = 0$.

The problem just solved can be regarded as a first approximation for the flow of a simple fluid which perturbs the rest state. Suppose the driving data for the slot flow described above are given by

$$T\langle xy\rangle(x,0) = \epsilon\tau(x).$$

There is no flow when $\epsilon = 0$. The equations of motion are

$$\rho(\boldsymbol{u}\cdot\nabla)\boldsymbol{u} = \nabla\cdot\boldsymbol{T}$$

$$\boldsymbol{u} = (u,v) = (\Psi_y, -\Psi_x)$$

$$\Psi(x,0,\epsilon) = \Psi(\pm 1,y,\epsilon) = \Psi_x(\pm 1,y,\epsilon) = \Psi(x,-\infty,\epsilon) = 0$$

$$T\langle xy\rangle(x,0,\epsilon) = \epsilon\tau(x), \tag{A.6}$$

where

$$\boldsymbol{T} = \left[-\Phi + \alpha_2(\gamma^2+\delta^2)\right]\boldsymbol{I} + \mu\boldsymbol{A} + \alpha_1\boldsymbol{B} + \mathrm{O}(\|\boldsymbol{u}\|^3),$$

$$\boldsymbol{A}[\boldsymbol{u}] \overset{\text{def}}{=} \boldsymbol{A}_1 \text{ is linear in } \boldsymbol{u},$$

$$\boldsymbol{B}[\boldsymbol{u},\boldsymbol{u}] \overset{\text{def}}{=} \boldsymbol{A}_2 \text{ is quadratic in } \boldsymbol{u}, \tag{A.7}$$

and γ, δ; the components of $\boldsymbol{A}$ and $\boldsymbol{B}$, are defined in terms of the stream function (with $\hat{}$ deleted) by (1.3).

Now we expand the solution in powers of ϵ

$$\begin{bmatrix} \Psi(x,y,\epsilon) \\ \boldsymbol{u}(x,y,\epsilon) \\ \Phi(x,y,\epsilon) \\ \boldsymbol{T}(x,y,\epsilon) \end{bmatrix} = \sum_{n=0}^{\infty} \epsilon^{n+1} \begin{bmatrix} \Psi_n(x,y) \\ \boldsymbol{u}_n(x,y) \\ \Phi_n(x,y) \\ \boldsymbol{T}_n(x,y) \end{bmatrix},$$

where

$$\boldsymbol{T}_0 = -\Phi_0\boldsymbol{I} + \mu\boldsymbol{A}[\boldsymbol{u}_0],$$

$$\boldsymbol{T}_1 = -\Phi_1\boldsymbol{I} + \mu\boldsymbol{A}[\boldsymbol{u}_1] + \alpha_1\boldsymbol{B}[\boldsymbol{u}_0,\boldsymbol{u}_0] + \alpha_2\boldsymbol{A}^2[\boldsymbol{u}_0],$$

$$\boldsymbol{A}^2[\boldsymbol{u}_0] = (\delta_0^2+\gamma_0^2)\boldsymbol{I},$$

$$\delta_0 = 2\Psi_{0,xy},$$

$$\gamma_0 = \Psi_{0,yy} - \Psi_{0,xx},$$

$$(\boldsymbol{T}_0)_{xy} = \mu\gamma_0,$$

$$(\boldsymbol{T}_1)_{xy} = \mu(\Psi_{1,yy} - \Psi_{1,xx}) + \alpha_1\left\{\left[\Psi_{0,y}\frac{\partial}{\partial x} - \Psi_{0,x}\frac{\partial}{\partial y}\right]\gamma_0 + \delta_0\nabla^2\Psi_0\right\} \tag{A.8}$$

At first order

$$0 = -\nabla \Phi_0 + \mu \nabla^2 \boldsymbol{u}_0,$$

$$\boldsymbol{u}_0 = (\Psi_{0,y'} - \Psi_{0,x})$$

$$\nabla^4 \Psi_0 = 0,$$

$$\Psi_0(x,0) = \Psi_0(\pm 1, y) = \Psi_{0,x}(\pm 1, y) = \Psi_0(x, -\infty) = 0,$$

$$\mu \Psi_{0,yy}(x,0) = \tau(x). \tag{A.9}$$

This is the linear problem solved by (A.5) with $f(x) = \tau(x)/\mu$ and Φ_0 is the Newtonian pressure. At second order we find that

$$\rho(\boldsymbol{u}_0 \cdot \nabla)\boldsymbol{u}_0 = -\nabla \Phi_1 + \mu \nabla^2 \boldsymbol{u}_1 + \nabla \cdot \{\alpha_1 \boldsymbol{B}[\boldsymbol{u}_0, \boldsymbol{u}_0] + \alpha_2 \boldsymbol{A}^2[\boldsymbol{u}_0]\}, \tag{A.10}$$

$$\boldsymbol{u}_1 = (\Psi_{1,y'} - \Psi_{1,x}),$$

$$\Psi_1(x,0) = \Psi_1(\pm 1, y) = \Psi_{1,x}(\pm 1, y) = \Psi_1(x, -\infty) = 0 \tag{A.11}$$

$$(\boldsymbol{T}_1)_{xy} = 0 \quad \text{on } y = 0; \quad \text{that is}$$

$$\mu \Psi_{1,yy} = -\alpha_1 \{[\Psi_{0,y} \gamma_{0,x} - \Psi_{0,x} \gamma_{0,y}] + \delta_0 \nabla^2 \Psi_0\}$$

$$\overset{\text{def}}{=} -\alpha_1 g(x). \tag{A.12}$$

A theorem of Giesekus [27] states that if div $\boldsymbol{A}[\boldsymbol{u}] = \text{grad } \tilde{\Phi}$ and div $\boldsymbol{u} = 0$ then

$$\text{div}(\boldsymbol{B}[\boldsymbol{u}, \boldsymbol{u}] - \boldsymbol{A}^2[\boldsymbol{u}]) = \text{grad}\left(\frac{\mathrm{d}\tilde{\Phi}}{\mathrm{d}t} + \frac{1}{2} \text{ tr } \boldsymbol{A}^2\right).$$

Applying this theorem to the last term of (A.10) and using $(A.8)_3$ we get

$$\rho(\boldsymbol{u}_0 \cdot \nabla)\boldsymbol{u}_0 = \nabla\left[-\Phi_1 + \frac{\alpha_1}{\mu}\frac{\mathrm{d}\Phi_0}{\mathrm{d}t} + \left(\alpha_2 + \frac{3\alpha_1}{2}\right)(\gamma_0^2 + \delta_0^2)\right] + \mu \nabla^2 \boldsymbol{u}_1. \tag{A.13}$$

If inertia is now neglected then $\nabla^4 \Psi_1 = 0$ and Ψ_1 is given by (A.5) with $f(x)$ replaced by $-\alpha_1 g(x)/\mu$ and Φ_1 is determined by the reduced form of (A.13) with the left side set to zero.

Let us suppose that $\tau(x) = \tau(-x)$ is symmetric. Then $\Psi_0(x,y) = \Psi_0(-x,y)$ and $\Phi_0(-x) = -\Phi_0(x)$. Now $\Psi_1(x,y)$ is determined by the driving data $g(x)$ in (A.12) and $g(-x) = -g(x)$, hence $\Psi_1(-x,y) = -\Psi_1(x,y)$. So the streamlines at first order are symmetric but the streamlines at second order are antisymmetric. So in this problem we do not get symmetric streamlines even if inertia is neglected.

This work was supported in part by the U.S. Army Research Office and under a grant from the Fluid Mechanics Division of NSF.

References

1 R.I. Tanner, Phys. Fluids, 9 (1966) 1246.
2 R.R. Huilgol, SIAM J. Appl. Math., 24 (1973) 226.
3 A.C. Pipkin and R.I. Tanner, in: S. Nemat-Nasser (Ed.), Mechanics Today, Vol. I, Pergamon, Oxford, 1974, p. 262.
4 R.I. Tanner and A.C. Pipkin, Trans. Soc. Rheol., 13 (1969) 1.
5 J.M. Broadbent, A. Kaye, A.S. Lodge and D.G. Vale, Nature, 217 (1968) 55.
6 A.S. Lodge, Patent No. 3777549 (1973), U.S. Patent Office.
7 T.H. Hou, P.P. Tong and L. DeVargas, Rheol. Acta, 16 (1977) 544.
8 C.D. Han and H.J. Yoo, J. Rheol., 24 (1980) 55.
9 V. O'Brien, Phys. Fluids, 15 (1972) 2089.
10 P. Townsend, Rheol. Acta, 19 (1980) 1.
11 D.S. Malkus, in: C. Klason and J. Kubát (Eds.), Proceedings of the VIIth International Congress on Rheology, Gothenberg, Sweden, 1976, p. 618.
12 A. Mir-Mohamad-Sadegh and K.R. Rajagopal, J. Appl. Mech., 47 (1980) 485.
13 T. Cochrane, K. Walters and M.F. Webster, Phil. Trans. Roy. Soc., 301 (1981) 163.
14 J. Sanders, V. O'Brien and D.D. Joseph, J. Appl. Mech., 47 (1980) 482.
15 D.D. Joseph and L. Sturges, J. Fluid Mech., 69 (1975) 565.
16 D.D. Joseph and L. Sturges, SIAM J. Appl. Math., 34 (1978) 7.
17 R.C.T. Smith, Austral. J. Sci. Res., 5 (1952) 227.
18 D.D. Joseph, in: H. Zorski (ed.), Trends in Applications of Pure Mathematics to Mechanics, Vol. II, Pitman, London, 1979, p. 129.
19 R.D. Gregory, Tech. Report No. 78-37, The Institute of Applied Mathematics and Statistics, The University of British Columbia, Vancouver, Canada, 1978.
20 R.D. Gregory, Tech. Report No. 79-23, The Institute of Applied Mathematics and Statistics, The University of British Columbia, Vancouver, Canada, 1979.
21 R.D. Gregory, J. Elasticity, 9 (1979) 1.
22 D. Spence, MRC-Wisconsin Report #1863, 1978.
23 M. Zidan, Rheol. Acta, 8 (1969) 89.
24 L.D. Sturges, Ph.D. Thesis, University of Minnesota, 1977.
25 S.A. Trogdon and D.D. Joseph, Rheol. Acta, 19 (1980) 404.
26 S.A. Trogdon, Ph.D. Thesis, University of Minnesota, 1981.
27 H. Giesekus, Rheol. Acta, 3 (1963) 59.